Proc. Natl. Acad. Sci. USA
Vol. 84, pp. 4475–4479, July 1987
Cell Biology

Visualization of Ca^{2+}-induced phospholipid domains*

(fluorescence microscopy/digital-image analysis/erythrocytes)

DORIS M. HAVERSTICK AND MICHAEL GLASER†

Department of Biochemistry, University of Illinois, Urbana, IL 61801

Communicated by Gregorio Weber, January 30, 1987

ABSTRACT **Large vesicles (5–15 μm) were formed by hydrating a dried lipid film containing phospholipids labeled with a fluorophore in one fatty acid chain. By using a fluorescence microscope attached to a low-light-intensity charge-coupled-device camera and digital-image processor, the vesicles were easily viewed and initially showed uniform fluorescence intensity across the surface. The fluorescence pattern of vesicles made with a fluorophore attached to phosphatidylcholine or phosphatidylethanolamine was unaffected by the presence of divalent cations such as Ca^{2+}, Mg^{2+}, Mn^{2+}, Zn^{2+}, or Cd^{2+}. The fluorescence pattern of vesicles containing a fluorophore attached to the acidic phospholipids phosphatidylserine or phosphatidic acid showed distinct differences when treated with Ca^{2+} or Cd^{2+}, although they were unaffected by Mg^{2+}, Mn^{2+}, or Zn^{2+}. Treatment with 2.0 mM Ca^{2+} or Cd^{2+} resulted in the movement of the fluorophore to a single large patch on the surface of the vesicle. When vesicles were formed in the presence of 33 mol % cholesterol, patching was seen at a slightly lower Ca^{2+} concentration (1.0 mM). The possibility of interactions between Ca^{2+} and acidic phospholipids in plasma membranes was investigated by labeling erythrocytes and erythrocyte ghosts with fluorescent phosphatidic acid. When Ca^{2+} was added, multiple (five or six) small patches were seen per individual cell. The same pattern was observed when vesicles formed from whole lipid extracts of erythrocytes were labeled with fluorescent phosphatidic acid and then treated with Ca^{2+}. This shows that the size and distribution of the Ca^{2+}-induced domains depend on phospholipid composition.**

Current knowledge of biological functions associated with cell membranes suggests that membranes are dynamic mobile structures with components capable of lateral movement and reorganization (1, 2). Perhaps the most striking example of membrane reorganization occurs during membrane aggregation and fusion, a process that mediates such important biological functions as exocytosis, fertilization, and intracellular transport. Of particular importance in many of these biological functions appears to be the interaction of divalent cations, particularly Ca^{2+}, with acidic phospholipids such as phosphatidic acid and phosphatidylserine. This is exemplified by the central role of Ca^{2+} in neurotransmitter release at presynaptic nerve terminals (3).

From use of model membrane systems and a variety of experimental approaches (4), there now exists a great deal of evidence for the formation of Ca^{2+}–acidic phospholipid complexes as a critical step in membrane fusion (5, 6). Studies on the kinetics of cation-induced vesicle aggregation and release of vesicle contents, coupled with x-ray diffraction and equilibrium dialysis binding studies, have suggested the formation of an intermediate Ca^{2+}–acidic phospholipid complex as a first step in vesicle fusion (6–8). Other laboratories have demonstrated the immobilization of acidic phospholipids by Ca^{2+} and the formation of a lateral phase separation in model membrane systems (9–13). Cd^{2+} forms tighter complexes with acidic phospholipids than does Ca^{2+}, while most other divalent cations are not effective (13, 14).

To date, direct visualization of such Ca^{2+}–phospholipid complexes has not been possible, although there has been some success in visualization of lipid phase separations (15, 16). For example, using lipid monolayers, McConnell and coworkers (16) visualized phase separations after compression of fluorescent phospholipids at an air/water interface. In experiments designed to study antibody-induced membrane events, Schroit and Pagano (17) were able to visualize capping in lymphoma cells, using an anti-phospholipid antibody and a modified phospholipid, trinitrophenylated phosphatidylethanolamine.

Through use of a combination of extremely large-diameter phospholipid vesicles, fluorescence microscopy, and computerized image analysis, the direct visualization of Ca^{2+}–phospholipid domain formation is demonstrated in this report. In addition, the techniques have been applied to a simple cell system, rabbit erythrocytes, with subsequent demonstration of similar domain formation within the plasma membrane.

MATERIALS AND METHODS

Fluorescent Phospholipids. 1-Acyl-2-[*N*-(4-nitrobenzo-2-oxa-1,3-diazole)aminocaproyl]-labeled phosphatidylcholine (NBD-phosphatidylcholine) and NBD-phosphatidylethanolamine were purchased from Avanti Polar Lipids. NBD-phosphatidic acid was prepared from NBD-phosphatidylcholine by enzymatic digestion with cabbage phospholipase D (Sigma) by the procedure of Yang *et al.* (18) as modified by Comfurius and Zwaal (19). After total lipid extraction of the reaction mixture (20), NBD-phosphatidic acid was purified by TLC on silica gel G plates (Analtech, Newark, DE) with $CHCl_3/CH_3OH/H_2O$, 65:25:4 (vol/vol), as the solvent (solvent I) and was eluted from the gel with acidic 50:100:5 $CHCl_3/CH_3OH/H_2O$ (solvent II). NBD-phosphatidylserine was prepared by transphosphatidylation with cabbage phospholipase D (18, 19). NBD-phosphatidylserine was purified by lipid extraction and TLC as above except that the solvent system was $CHCl_3/CH_3OH/NH_4OH$, 65:40:5 (vol/vol), and the elution buffer was $CHCl_3/CH_3OH/NH_4OH$, 50:100:5.

N-(5-Dimethylaminonaphthalene-1-sulfonyl)aminoundecanoic acid (C_{11}-dansyl) was purchased from Molecular Probes (Junction City, OR). C_{11}-dansyl was attached to lysophosphatidylcholine (Sigma) by first treating the C_{11}-dansyl with *N,N'*-dicyclohexylcarbodiimide (Aldrich) for 1.5 hr with vigorous stirring in toluene and then mixing the reaction mixture with fully dehydrated lysophosphatidylcholine in the presence of sodium oxide. Toluene was evaporated in a Buchler Rotovapor R with the reaction vessel

The publication costs of this article were defrayed in part by page charge payment. This article must therefore be hereby marked "*advertisement*" in accordance with 18 U.S.C. §1734 solely to indicate this fact.

Abbreviations: NBD, 1-acyl-2-[*N*-(4-nitrobenzo-2-oxa-1,3-diazole)-aminocaproyl]; C_{11}-dansyl, *N*-(5-dimethylaminonaphthalene-1-sulfonyl)aminoundecanoic acid.

*A preliminary report of this work has been presented (32).

†To whom reprint requests should be addressed.

held in a 70°C oil bath. Product was isolated by TLC on silica gel G plates with solvent I followed by elution from the silica with solvent II. C_{11}-dansyl-conjugated phosphatidic acid was synthesized from C_{11}-dansyl-phosphatidylcholine as outlined above for NBD-phosphatidic acid.

Dioleoyl phosphatidylcholine and cholesterol were purchased from Sigma. Phospholipid concentrations were based on phosphate content determined after perchloric acid digestion using the Ames procedure (21). All phospholipids were stored at −20°C in either $CHCl_3$ or toluene and were routinely checked by TLC for purity.

Vesicle Formation. Large unilamellar vesicles for viewing were formed according to Darszon *et al.* (22). Vesicles for use in labeling cells were prepared by the ethanol injection procedure of Kremer *et al.* (23) in 10 mM *N*-2-hydroxyethylpiperazine-*N'*-2-ethanesulfonic acid/150 mM NaCl, pH 7.4, with 0.04% sodium azide.

Erythrocyte Isolation. Whole blood was obtained from the ear vein of a New Zealand rabbit and mixed with 0.2 volume of 39 mM citric acid/75 mM trisodium citrate/135 mM glucose, pH 4.5. The blood was centrifuged at 160 × *g* for 15 min to remove the platelet-rich plasma. A further 0.2 volume of citrate buffer was added, and the suspension was centrifuged at 1300 × *g* for 10 min. The clear supernatant was removed, and the erythrocytes were diluted to 20,000–40,000 per μl in 10 mM Tris/150 mM NaCl, pH 7.4 (TBS). Cells were used for 12 hr and then discarded.

Ghost Preparation. Erythrocyte ghosts were prepared by the method of Lee *et al.* (24) and were suspended in TBS.

Slide Preparation. *Vesicles.* To be able to view a single phospholipid vesicle over time, it was necessary to immobilize the vesicles in agarose on the microscope slide. In addition, this prevented vesicle aggregation. Briefly, vesicle preparations were mixed with the appropriate cation at the various concentrations, and 5 μl were immediately pipetted onto a microscope slide and mixed with 5 μl of 0.25% agarose at 40°C. A cover slip was applied, and the slide was cooled to 20°C within 15 sec. A single vesicle or population of vesicles was located within 2 min, and an image was captured (see description of instrumentation below). The sample was not illuminated between time points to prevent excessive bleaching of the fluorophore.

Cells. Erythrocytes and ghosts (5 μl) were pipetted directly onto the microscope slide, and a cover slip was applied with slight pressure to decrease the movement of the cells while viewing. The experiments involving mixing of erythrocytes or ghosts with cations were carried out as described above for the vesicles.

Instrumentation. The instrument was constructed with a Leitz microscope made entirely with quartz optics and using epifluorescence illumination. A xenon arc lamp was used as the light source. The image was sensed by a charge-coupled-device video camera (with image intensifier) from ITT-Fairchild (Palo Alto, CA) and was fed into an IBM 9000 computer modified by Quantex (Sunnyvale, CA) for digital-image processing. The image was visualized on a Sony 13-inch color monitor, and photographs were taken directly off the monitor screen. By using the image-processing program, 200 frames were averaged in real time (30 frames per sec) to decrease background and electrical noise. To visualize more clearly changes in distribution and intensity of the fluorophores, a pseudo-color program was applied to all images. In essence, the 256 gray tones (black = 1; white = 256) used by the image processor were assigned color values from dark blue to light blue to green to yellow to red (see Fig. 1). The instrumentation will be described in detail elsewhere.

RESULTS

Phospholipid Vesicles. Fig. 1 shows typical phospholipid vesicles as seen under epifluorescent illumination by the video camera and analyzed by the computer. To be visible, the vesicles had to be made with a fluorescent phospholipid. Fig. 1*E* shows the color overlay scheme that the Quantex program has applied to the averaged picture. This color scheme gives an artifactual edging effect when going from one color to another. For example, in Fig. 1*A*, the edge of the vesicle corresponds to the outer edge of the dark green ring. For phosphatidylcholine vesicles containing either 1% fluorescent phosphatidic acid or 1% fluorescent phosphatidylcholine, there was no apparent change in intensity or shape of the immobilized phospholipid vesicles during the experimental period (Fig. 1 *A* and *B*). Measurements of radiance levels across the surface of the vesicles showed no change at the various time points (data not shown). Fig. 1 *C* and *D* show similar vesicles incubated in the presence of 2 mM $CaCl_2$. Fig. 1*D* shows the absence of an effect by Ca^{2+} on the fluorescent phosphatidylcholine, while Fig. 1*C* shows that in

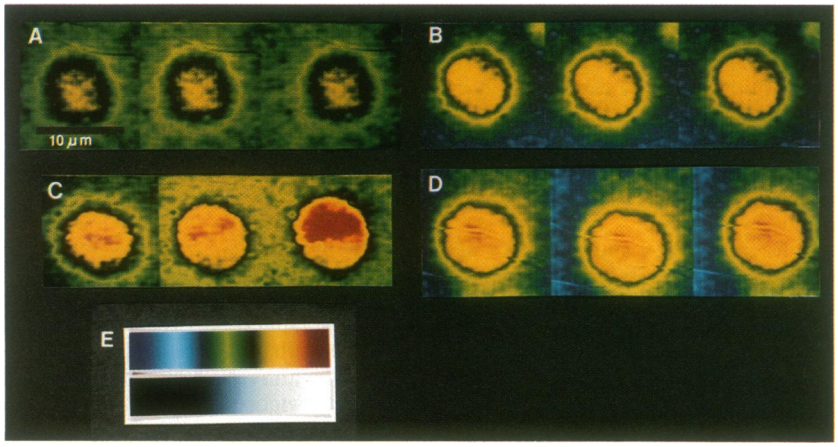

FIG. 1. Effect of Ca^{2+} on phospholipid vesicles. (*A*) Vesicles made from a dioleoyl phosphatidylcholine/NBD-phosphatidic acid mixture, 99:1 mol %, were used as the starting material. A single vesicle was found in the camera field and monitored at 2 (*Left*), 15 (*Center*), and 30 (*Right*) min. (*B*) A similar vesicle, but hydrated from a dioleoyl phosphatidylcholine/NBD-phosphatidylcholine mixture (99:1 mol %) viewed at the same time points as in *A*. (*C*) A vesicle such as described in *A*, viewed at 2, 15, and 30 min in the presence of 2.0 mM $CaCl_2$ added at zero time. (*D*) A vesicle as in *B*, viewed at the same time points as in *C* in the presence of 2.0 mM $CaCl_2$ added at zero time. (*E*) Representation of the pseudo-color program (*Upper*) applied to the gray tones (*Lower*) viewed by the video camera. Notice the artifactual edging effect caused by the blending of successive colors.

the presence of Ca^{2+}, one portion of the vesicle has been enriched in fluorescent phosphatidic acid. Results similar to those seen in Fig. 1*C* were found when fluorescent phosphatidylserine vesicles were used (i.e., sequestering in the presence of Ca^{2+}). Vesicles made with fluorescent phosphatidylethanolamine were unaffected by addition of Ca^{2+}. There were no differences seen when C_{11}-dansyl-conjugated phospholipids were used rather than NBD-phospholipids (data not shown).

In an effort to determine how specific the interaction of phosphatidylserine or phosphatidic acid with Ca^{2+} was, vesicles made with either fluorescent phosphatidylserine, phosphatidic acid, phosphatidylcholine, or phosphatidylethanolamine were incubated with a variety of cations. The results are tabulated in Table 1. A minimum of 10 fields of vesicles was viewed for each condition. Of the cations tested, only Ca^{2+} and Cd^{2+} were effective at the concentrations used and only for vesicles made up with phosphatidic acid or phosphatidylserine. Under no circumstances was there reorganization within vesicles made up with phosphatidylcholine or phosphatidylethanolamine as the fluorescent phospholipid.

Since many biological membranes contain a large percentage of cholesterol, the effect of the substitution of some of the dioleoyl phosphatidylcholine by cholesterol (33 mol %) on the phosphatidic acid–Ca^{2+} interaction was assessed. Vesicles made up with dioleoyl phosphatidylcholine and NBD-phosphatidic acid only were unaffected by 0.5 mM (Fig. 2*A*) or 1.0 mM (Fig. 2*C*) $CaCl_2$. Radiance measurements taken at 0 and 30 min confirm the lack of reorganization (data not shown). In the presence of 2.0 mM $CaCl_2$ (Fig. 2*E*), the phosphatidic acid was sequestered as seen in Fig. 1. When vesicles were made up with dioleoyl phosphatidylcholine, NBD-phosphatidic acid, and cholesterol, however, the effective concentration of calcium was decreased to 1.0 mM (Fig. 2*D*). There was no visible difference in the degree of sequestering between the 1.0 and 2.0 mM Ca^{2+} conditions (Fig. 2 *D* and *F*, respectively), suggesting that the sequestering of phosphatidic acid in response to Ca^{2+} was an all or none phenomenon. It is of interest that the vesicles formed in the presence of cholesterol were somewhat larger than those formed in its absence. The vesicles in Fig. 2 *B* and *F* were 18–20 μm in diameter.

Erythrocytes. In an effort to determine if Ca^{2+}-induced domain formation would occur *in vivo*, rabbit erythrocytes were fluorescently labeled by the methods of Pagano *et al.* (25), which were developed for studies on transport and metabolism of phospholipids *in vivo*. The cells were incubated with ethanol-injected vesicles made from 25 mol % NBD-phosphatidic acid in dioleoyl phosphatidylcholine. This concentration of NBD-phosphatidic acid was chosen because these vesicles are too small to be seen and will not contribute greatly to the background fluorescence due to the self-quenching capacity of NBD at this concentration (26). After a 15-min 20°C incubation, the vesicle/cell suspension was centrifuged briefly (1000 × *g* for 5 min) to pellet the erythrocytes and to separate them from the vesicles. The erythrocytes were resuspended in TBS, and $CaCl_2$ was added to a final concentration of 10 mM. A slide was prepared and viewed over time. Fig. 3*A* shows the fluorescence image 2 min after the addition of Ca^{2+}, and Fig. 3*B* shows the same cells 10 min after Ca^{2+} addition. As can be seen, the erythrocytes were uniformly labeled at zero time, and they maintained their distinctive biconcave shape (Fig. 3*C*). After 10 min in the presence of Ca^{2+}, however, the fluorescence was unevenly distributed and could be seen as multiple small patches approximately 1 μm in diameter on the surface of the cell. The redistribution of fluorescence was not accompanied by any changes in cell shape (Fig. 3*D*). In addition, the redistribution was not dependent upon the initial level of label incorporated into the cells as seen in Fig. 3 *A* and *B* by the bright (*Left*) and dim (*Right*) cells. This same pattern of patching in the presence of divalent cations was seen when $CdCl_2$ was used, but not when $MgCl_2$ was used. In addition, there was no reorganization of fluorescence when the erythrocytes were labeled with NBD-phosphatidylcholine and then exposed to divalent cations (data not shown). Finally, to ensure that the patching was due to the same phosphatidic acid–Ca^{2+} interaction seen in the vesicles and that there was no metabolism of the fluorescent phosphatidic acid as has been reported by others for different types of cells (27), the total lipid fraction was extracted from NBD-phosphatidic acid-labeled erythrocytes before and after the addition of Ca^{2+} (20). The extracted lipids were run on TLC plates. The fluorescence in the erythrocyte lipid extract migrated as a single spot and for the same distance as the starting compound, NBD-phosphatidic acid. These results show that the patching seen in Fig. 3*B* was in fact due to the specific interactions of Ca^{2+} and phosphatidic acid.

Because the pattern of patching seen in the erythrocytes was different from that seen in the phospholipid vesicles (Figs. 1 and 2), two additional experiments were carried out. In the first, erythrocyte ghosts were prepared from fresh erythrocytes and were labeled with NBD-phosphatidic acid (Fig. 3*E*). After the addition of $CaCl_2$ (10 mM), the fluorescence pattern changed from uniform to multiple small patches (Fig. 3*F*). In the next experiment, when vesicles were formed from a total lipid extract of erythrocytes, labeled with NBD-phosphatidic acid (Fig. 3*G*), and then treated with 10 mM $CaCl_2$ (Fig. 3*H*), the same multiple small patches were seen as in the intact cells and ghosts. Again, the initial level of fluorescence labeling had no effect on the pattern of fluorescence that developed in the presence of Ca^{2+}. These results strongly suggest that the different phospholipids in the erythrocyte plasma membrane were responsible for the different patterns of domain formation and not the membrane proteins or the cytoskeleton.

Table 1. Effect of cations on phospholipid domain formation

Conditions	PtdOH	PtdSer	PtdCho	PtdEtn
$CaCl_2$	+	+	–	–
$MgCl_2$	–	–	–	–
$MnCl_2$	–	–	–	–
$CdCl_2$	+	+	–	–
$ZnCl_2$	–	–	–	–

Vesicles were incubated for 30 min in the presence of 2 mM of the indicated salt. Reorganization of the fluorescent phospholipid is indicated by "+". Vesicles that were unaffected by the addition of salt are indicated by "–." A minimum of 10 fields was examined for each condition. All vesicles were labeled with 1 mol % NBD-phospholipid in dioleoyl phosphatidylcholine. PtdOH, phosphatidic acid; PtdSer, phosphatidylserine; PtdCho, phosphatidylcholine; PtdEtn, phosphatidylethanolamine.

DISCUSSION

Lateral molecular mobility within cell membranes and artificial bilayer systems has been studied extensively by a variety of methods. One of the most dramatic examples of membrane reorganization occurs when two previously isolated and distinct membranes fuse to form a new boundary membrane. Membrane fusion occurs as a highly regulated step in many biological processes such as exocytosis, fertilization, and intracellular transport (1). In an effort to better understand the molecular events involved in fusion, phospholipid model systems have been used with some success (4). One important finding to come out of such work has been the critical role the interaction of acidic phospholipids and certain divalent cations have in promoting bilayer fusion. It

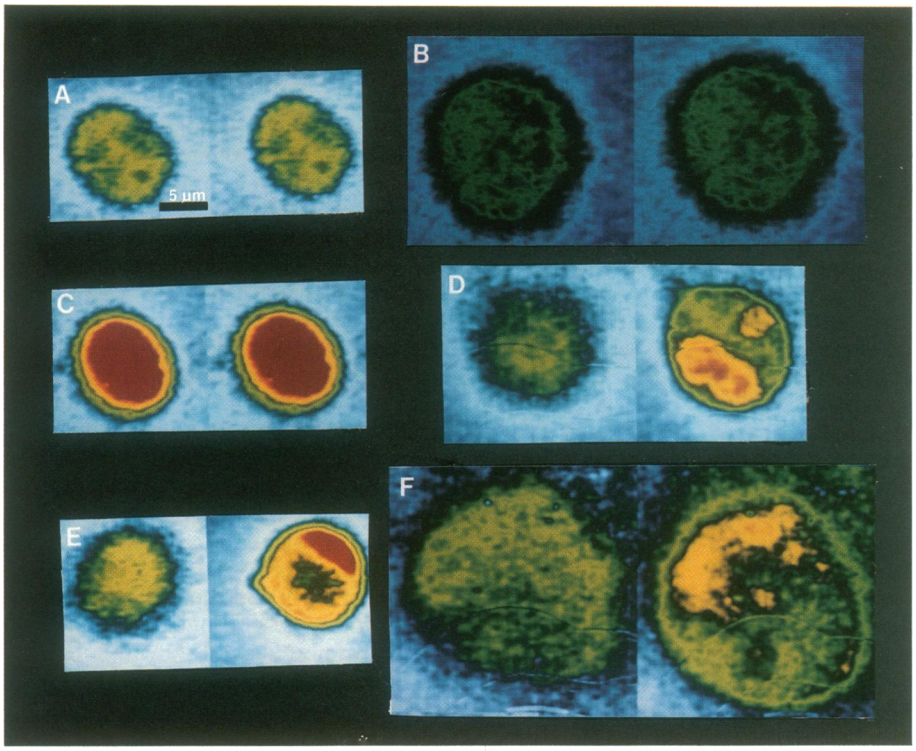

FIG. 2. Effect of cholesterol on Ca^{2+}–phosphatidic acid interactions in incubations with $CaCl_2$ at 0.5 (*A* and *B*), 1.0 (*C* and *D*), and 2.0 (*E* and *F*) mM. (*A*, *C*, and *E*) Vesicles were hydrated from dioleoyl phosphatidylcholine/NBD-phosphatidic acid (99.5:0.5 mol %). (*B*, *D*, and *F*) Vesicles were made from dioleoyl phosphatidylcholine/NBD-phosphatidic acid:cholesterol (66.5:0.5:33 mol %). (*A–F Left*) Image of the vesicle at 2 min. (*A–F Right*) Image after 30 min of incubation in the presence of $CaCl_2$.

has been postulated that Ca^{2+} may have a regulatory role in fusion as well as an active role by sequestering acidic phospholipids as an early step in the process (8). Another example of such a dual role occurs when Ca^{2+} is released from platelets in an early step in blood clotting (28).

With the large (8- to 15-μm) vesicles that have been used

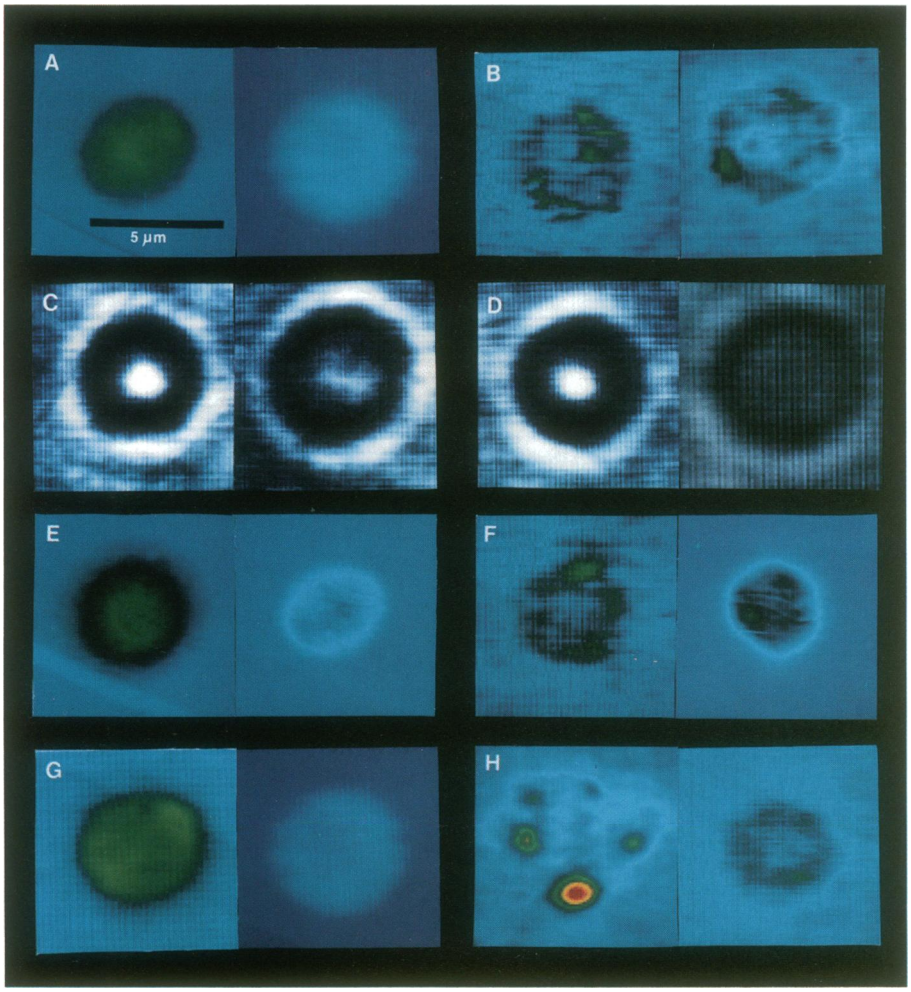

FIG. 3. Effect of Ca^{2+} on rabbit erythrocytes labeled with fluorescent phosphatidic acid. (*A–D*) Isolated rat erythrocytes (200 μl) were incubated with ethanol-injected vesicles (20 μl of 25 mol % NBD-phosphatidic acid in dioleoyl phosphatidylcholine; 500 nmol of phospholipid/ml) for 15 min at 20°C and were centrifuged (1000 × *g* for 5 min). Cells were resuspended in TBS. Slides were prepared and viewed at 2 (*A* and *C*) and 10 (*B* and *D*) min after the addition of 10 mM $CaCl_2$ using epifluorescence (*A* and *B*) and transmitted light (*C* and *D*). (*E* and *F*) Erythrocyte ghosts were prepared and labeled as described for the erythrocytes. Slides were prepared and viewed at 2 (*E*) and 10 (*F*) min after the addition of 10 mM $CaCl_2$. (*G* and *H*) Lipids were extracted from fresh erythrocytes (20) and used to form vesicles. Extracted phospholipids (498 nmol) and NBD-phosphatidic acid (3 nmol) were dried down, and vesicles were formed in 1 ml of H_2O. Vesicles were viewed at 2 (*G*) and 30 (*H*) min after the addition of 2 mM $CaCl_2$. Examples of both brightly labeled (*A–H Left*) and dimly labeled (*A–H Right*) cells and vesicles are shown to demonstrate that the initial level of label did not affect the changes in fluorescence patterns after the addition of Ca^{2+}.

for the studies presented here, it now becomes possible to visualize such cation-induced domains as they are formed along the phospholipid bilayer. In addition, by immobilizing the vesicles immediately after the addition of cations, it is possible to separate the molecular events of bilayer reorganization from those associated with aggregation or fusion. The cation and phospholipid specificities of domain formation seen here are in good agreement with the requirements for lipid-phase separation and liposome fusion (5, 7, 14). As outlined in Table 1, the formation of visible domains occurred only when the acidic phospholipids phosphatidic acid and phosphatidylserine were exposed to Ca^{2+} or Cd^{2+}. It is also clear from Table 1 that the neutral charged phospholipids phosphatidylcholine and phosphatidylethanolamine were not sequestered by the cations.

The Ca^{2+}-induced phosphatidic acid domains were clearly not pure phosphatidic acid because the domains encompassed roughly 50% of the vesicle's surface, while the vesicles contained only a few percent of phosphatidic acid. This suggests that a complete separation of the two phospholipids was not occurring. Complete quantitation of all aspects of the domains formed using these vesicles was not possible because of the self-quenching properties of NBD (25).

The effects of cholesterol on phospholipid membranes have been extensively investigated. Cholesterol decreases the surface area per molecule occupied by phospholipids through a condensing effect on phospholipid packing (29). Decreased surface area could explain the increased sensitivity to Ca^{2+} exhibited by vesicles formed in the presence of cholesterol as demonstrated in Fig. 2. If cholesterol has decreased the distance between phosphatidic acid molecules, it is conceivable that it would take less Ca^{2+} to form the complex that results in patching of the fluorescent phosphatidic acid (Fig. 2*D*).

Although calcium did induce domain formation of acidic phospholipids in both phospholipid vesicles and erythrocytes, the sizes of the domains were different. Based on the results of the experiments shown in Fig. 3, it seems that the differences in phospholipid composition of the vesicles are responsible for the different fluorescence patterns seen and not membrane proteins. In addition to phospholipid headgroup differences between the different types of vesicles, there were differences in the acyl-chain length, degree of saturation, and cholesterol content. The presence of cholesterol did not seem to influence the size of the domains but only the Ca^{2+} concentration at which they occurred (Fig. 2). The other factors need further evaluation.

Despite the differences in the patterns of fluorescence after Ca^{2+} treatment, it is clear that domain formation is being viewed in the erythrocytes. The concentration of Ca^{2+} used for these studies is close to that seen in whole blood (30) and is below that sequestered in mitochondria (31), for example. It seems likely that such domains may form in biological membranes and be important in biological processes.

We thank Dr. Gregorio Weber and Dr. John Eklund for designing and building the microscope. We also thank Joe Cimino and Dag Zapatero for assistance in the synthesis of the fluorescent phospholipids and Jean Lewis for preparation of the manuscript. This work was supported by National Institutes of Health Grant GM 21953 (to M.G.). Funds for construction of the microscope were provided in part by National Institutes of Health Grant GM 11223 (to G. Weber).

1. Edidin, R. (1974) *Annu. Rev. Bioeng.* **3,** 179–201.
2. Singer, S. J. (1974) *Annu. Rev. Biochem.* **43,** 805–833.
3. Poste, G. & Allison, A. C. (1973) *Biochim. Biophys. Acta* **300,** 421–465.
4. Rand, R. P. & Parsegian, V. A. (1986) *Annu. Rev. Physiol.* **48,** 201–212.
5. Morris, S. J., Gibson, C. C., Smith, P. D., Greif, P. C., Stirk, C. W., Bradley, D., Haynes, D. H. & Blumenthal, R. (1985) *J. Biol. Chem.* **260,** 4122–4127.
6. Portis, A., Newton, C., Pangborn, W. & Papahadjopoulos, D. (1979) *Biochemistry* **18,** 780–790.
7. Newton, C., Pangborn, W., Nir, S. & Papahadjopoulos, D. (1978) *Biochim. Biophys. Acta* **506,** 281–287.
8. Papahadjopoulos, D., Vail, W. J., Newton, C., Nir, S., Jacobson, K., Poste, G. & Lazo, R. (1977) *Biochim. Biophys. Acta* **465,** 579–598.
9. Hoekstra, D. (1982) *Biochemistry* **21,** 2833–2840.
10. Ito, T., Ohnishi, S., Ishinaga, M. & Kito, M. (1975) *Biochemistry* **14,** 3064–3069.
11. Van Dijck, P. W. M., de Kruijff, B., Verkleij, A. J., Van Deenen, L. L. M. & de Gier, J. (1978) *Biochim. Biophys. Acta* **512,** 84–96.
12. Tanaka, Y. & Schroit, A. J. (1986) *Biochemistry* **25,** 2141–2148.
13. Feigenson, G. W. (1983) *Biochemistry* **22,** 3106–3112.
14. Feigenson, G. W. (1982) *Biophys. J.* **37,** 165.
15. Peters, R. & Beck, K. (1983) *Proc. Natl. Acad. Sci. USA* **80,** 7183–7187.
16. McConnell, H. M., Tamm, L. K. & Weis, R. M. (1984) *Proc. Natl. Acad. Sci. USA* **81,** 3249–3253.
17. Schroit, A. J. & Pagano, R. E. (1981) *Cell* **23,** 105–112.
18. Yang, S. F., Freer, S. & Benson, A. A. (1967) *J. Biol. Chem.* **242,** 477–484.
19. Comfurius, P. & Zwaal, R. F. A. (1977) *Biochim. Biophys. Acta* **488,** 36–42.
20. Bligh, E. G. & Dyer, W. J. (1959) *Can. J. Biochem. Physiol.* **37,** 911–917.
21. Ames, B. N. & Dubin, D. T. (1960) *J. Biol. Chem.* **235,** 769–775.
22. Darszon, A., Vandenberg, C. A., Schonfeld, M., Ellisman, M. H., Spitzer, N. C. & Montal, M. (1980) *Proc. Natl. Acad. Sci. USA* **77,** 239–243.
23. Kremer, J. M. H., Esker, M. W. J., Pathmamanoharan, C. & Wiersema, P. H. (1977) *Biochemistry* **16,** 3932–3935.
24. Lee, B., McKenna, K. & Bramhill, J. (1985) *Biochim. Biophys. Acta* **815,** 128–134.
25. Pagano, R. E., Longmuir, K. J. & Martin, O. C. (1983) *J. Biol. Chem.* **258,** 2034–2040.
26. Nichols, J. W. & Pagano, R. E. (1981) *Biochemistry* **20,** 2783–2789.
27. Pagano, R. E., Longmuir, K. J., Martin, O. C. & Stuck, D. K. (1981) *J. Cell Biol.* **91,** 872–877.
28. Berndt, M. C. & Phillips, D. R. (1981) in *Platelets in Biology and Pathology 2*, eds. Dingle, J. T. & Gordon, J. L. (Elsevier/North Holland, Amsterdam), pp. 43–75.
29. Yeagle, P. L. (1985) *Biochim. Biophys. Acta* **822,** 267–287.
30. Hao, Y. (1981) in *Handbook in Clinical Laboratory Science*, eds. Grenwalt, T. J. & Stearne, E. A. (CRC, Boca Raton, FL) Vol. II, p. 119.
31. Lehninger, A. L. (1970) *Biochem. J.* **119,** 129–138.
32. Haverstick, D. M. & Glaser, M. (1986) *J. Cell Biol.* **103,** 467a (abstr.).